Fibers and Polymers (2024) 25:331–346
https://doi.org/10.1007/s12221-023-00424-0

Online ISSN 1875-0052
Print ISSN 1229-9197

REGULAR ARTICLE

# Mechanical, Thermal, Morphological, and Fibre Characteristics During Injection Moulding of Green Composites

**G. Surya Rao[1] · K. Debnath[1] · R. N. Mahapatra[1]**

Received: 19 July 2023 / Revised: 30 October 2023 / Accepted: 3 November 2023 / Published online: 3 December 2023
© The Author(s), under exclusive licence to the Korean Fiber Society 2023

**Abstract**
The current work demonstrates the mechanical, thermal, and morphological characteristics of green composites processed by injection moulding. Bamboo fibre (BF) was chemically treated with 2% sodium hydroxide (NaOH) for 4 h to develop eco-friendly bamboo fibre-reinforced polylactic acid (BF/PLA) composites. Initially, the effect of fabrication parameters namely fibre length (2, 3, 4, 5, and 6 mm) and fibre loading (10, 20, and 30 wt%) on the tensile and flexural properties of the BF/PLA composite was investigated. Then the effect of the injection parameters namely injection pressure (70, 90, and 110 bars), injection speed (40, 50, and 60 mm/s), and injection temperature (165, 175, and 185 °C) on the mechanical properties was investigated by evaluating the tensile, flexural, compression, and shear properties of the developed BF/PLA composite. The significance of the fabrication and injection parameters was statistically analyzed using the grey relation analysis (GRA) technique. The thermogravimetric analysis (TGA) and derivative thermogravimetric analysis (DTG) were also performed to investigate the thermal performance of the developed composites. Furthermore, the morphology of the mechanically failed specimens was studied using a Field-Emission Scanning Electron Microscope (FE-SEM). The fibre dispersion, fibre orientation, and fibre length retention were also investigated to assess the characteristics of fibre during injection moulding of the developed composites. The optimum injection parameters to achieve better mechanical properties were found as A2–B3–C1 (injection pressure: 90 bars, injection speed: 60 mm/s, and injection temperature: 165 °C). The thermal stability of pure PLA was found better than the BF (20%)/PLA composite. The original fibre length retention in the Rank 1 composite was 59.3%.

**Keywords** Bamboo fibre · Fibre length · Fibre loading · Injection parameters · Mechanical Properties · Thermal analysis · Morphology · Grey relational analysis · Fibre characteristics

## 1 Introduction

Sustainability is a major concern in present days because of the limited resources and adverse effects posed by synthetic composites. Much effort has been given to replacing synthetic composite with green composite. Green composites are contemplated as the next-generation materials that can satisfy global needs due to their sustainable characteristic. The surface modification of fibre and the selection of a suitable fabrication process are the key factors to develop high-quality green composites. Green composites have many applications in structural, packaging, marine, sports, electronics, and automotive industries. Joseph et al. [1] examined the influence of fibre loading and length on the mechanical characteristics of natural rubber-reinforced palm fibre-based injection-moulded green composite. The authors found that 6 mm was the optimum fibre length. The tensile strength of the green composite dropped as the fibre loading was increased. Negawo et al. [2] explored the role of fibre loading on the physical, mechanical, and morphological characteristics of ensete fibre-reinforced with HDPE. The composite consisted of 25% fibre loading had ultimate tensile strength and tensile modulus of 19.3 MPa and 2.15 GPa. The ultimate flexural strength and modulus were found as 44 MPa and 445 MPa, respectively. Arao et al. [3] evaluated the mechanical characteristics of short and long fibre pellets of a jute/PLA produced by twin-screw extruder supplemented by injection moulding. The short fibre pelletized composite performed better than long fibre pelletized composite. The twin-screw extruder helped to achieve proper fibre distribution throughout the green composite of jute/

✉ G. Surya Rao
suryaforever365@gmail.com

[1] Department of Mechanical Engineering, National Institute of Technology Meghalaya, Shillong 793 003, India

PLA. Lemaire et al. [4] studied the mechanical properties of miscanthus fibre/PHBV-based green composite by varying the fibre loading. The increment in fibre loading from 0 to 30% reduced the tensile strength by 23% compared to the neat PHBV matrix. Sirichalarmkul and Kaewpirom [5] studied the influence of rice husk (RH) content on the mechanical properties of RH/PLA/PBS-based injection-moulded composite. The tensile strength and modulus of PLA/RH 30% composite decreased by 19% and 29% when compared with pure PLA samples. However, percentage elongation and impact strength were improved by 55% and 7.1%. Barczewski et al. [6] analyzed the mechanical and morphological properties of sunflower husk/PP-based injection-moulded composite by varying the particle size and content. At 20% fibre loading, the peak tensile strength and modulus were 29.9 MPa and 1.30 GPa. Kucuk et al. [7] varied the content of kieselguhr (KG) in injection-moulded TPU-based green composites to improve their mechanical and thermal properties. The mechanical and thermal characteristics of TPU/KG-based composite were enhanced by 30% due to the inclusion of KG. The mechanical and thermal properties gradually deteriorated as the KG content increased further. Zindani et al. [8] examined the influence of short punica granatum fibre (SPGF) loading on the mechanical and physical characteristics of SPGF/bio-epoxy-based green composite. The ultimate tensile strength and modulus were 29.93 MPa and 3.2 GPa, at 30% SPGF fibre loading. However, the maximum flexural strength and modulus were found as 54.86 MPa and 4.46 GPa. Sun et al. [9] evaluated and compared the mechanical and thermal characteristics of a sisal/jute/PP-based injection-moulded composite at varying fibre loading. The tensile strength and modulus of PP/30% sisal fibre composite were increased by 56% and 147% as compared to neat PP. In addition, the flexural strength and modulus improved by 90% and 217%, respectively. The findings reveal that sisal fibre-based composites had higher thermal stability than jute fibre-based composites. Zhang et al. [10] explored the impact of injection parameters on the mechanical and morphological characteristics of injection-moulded PBS/PBAT/PHBV-miscanthus-based green composites. The optimal melting and mould temperatures were 165℃ and 45℃ to achieve better mechanical properties. Muthuraj et al. [11] investigated the effect of miscanthus fibre (MF) loading on the tensile, flexural, and impact properties of PBS/MF-based green composite. The addition of 50% MF improved the tensile, flexural, and impact strength by 22, 139, and 47% compared to neat PBS. Subyakto et al. [12] varied the fibre loading of bamboo and sisal fibre to examine the tensile and bending properties of PLA-based bio-composite. The composite of 30% SF/PLA attained ultimate tensile strength and modulus as 48.18 MPa and 1.13 GPa. Meanwhile, the maximum flexural strength and modulus were noticed as 67.83 MPa and 4.43 GPa. The maximum tensile strength and modulus of 20% BF/PLA-based green composite was 44.55 MPa and 1.2 GPa. The ultimate flexural strength and modulus were noted as 62.3 MPa and 3.89 GPa, respectively. Bax and Mussig [13] studied the mechanical characteristics of the injection-moulded PLA/cordenka fibre (CF) and PLA/flax fibre (FF)-based green composites by varying the fibre loading. Both the developed composites showed superior mechanical properties at 30% fibre loading. The ultimate tensile strength and modulus of PLA/CF were 57.94 MPa and 4.76 GPa. The maximum tensile strength and modulus were estimated as 54.15 MPa and 6.31 GPa for PLA/FF-based composite. Chaitanya and Singh [14] evaluated the mechanical performance of 30% sisal fibre/PLA composite fabricated by both direct injection and extrusion injection. The authors revealed that the direct injection was more suitable than the extrusion injection in attaining better mechanical properties. The short sisal fibre-based biocomposite showed improvement in tensile and flexural strengths at 34.7% and 15.9% through direct injection. Koffi et al. [15] investigated the effect of birch fibre loading on the tensile properties of injection-moulded HDPE-based composite. The addition of 40% birch fibre resulted in achieving the maximum tensile strength and modulus of 45.54 MPa and 4.39 GPa, respectively. The authors reported that more addition of birch fibre resulted in an increase in the composite stiffness. Aliotta et al. [16] studied the effect of fibre loading on the mechanical, thermal, and morphological properties of sisal fibre (SF)/PLA-based green composite developed by injection moulding. The addition of 20% SF helped to attain the maximum stress of 66 MPa for the SF/PLA composite. Moreover, PLA's glass transition temperature was enhanced up to the addition of 20% SF. Rodriguez et al. [17] optimized the influence of process parameters on the mechanical properties of banana fiber/PLA/HDPE-based green composites. The ultimate tensile strength of 27.74 MPa was achieved when the composite was developed using 37.95% banana fibre and 30/32.05% PLA/HDPE. Czerniecka-Kubicka et al. [18] studied the thermal and mechanical properties of hemp fibre/PHBV-based biocomposite. The inclusion of hemp fibre (HF) in the PHBV matrix improved the degree of crystallinity as compared to pure PHBV. The biocomposite of 30% HF/PHBV attained the maximum tensile strength and modulus of 42.90 MPa and 6.99 GPa, respectively. Dhakal et al. [19] investigated the tensile, impact, and morphological properties of date palm fibre/PCL-based green composite. The tensile strength and modulus were improved from 19 to 25 MPa and 140 to 282 MPa for the inclusion of 28% date palm fibre. Lekrine et al. [20] studied the influence of washingtonia filifera (WF) fibre loading on the mechanical, thermal, and physical properties of injection-moulded WF/HDPE-based green composite. A quick degradation of composite with the addition of 20% WF fibre was observed when compared with neat HDPE. The superior mechanical

and thermal properties were achieved in 20% WF/HDPE-based green composite.

The above literature clearly indicates that in-depth investigation is required to find the effect of fabrication and injection parameters on the mechanical characteristics of BF/PLA green composites as the mechanical performance of BF/PLA-based composites was not thoroughly studied. Thus, this study is an attempt to find the mechanical performance of the green composites affected by the fabrication parameters (fibre loading and length) and injection parameters (injection pressure, speed, and temperature). GRA was applied to find the optimum condition of fabrication parameters and injection parameters. The significance of the chosen parameters was also found by employing ANOVA. The morphological analysis of shattered composite specimens was examined to evaluate the failure behaviour under diverse loadings. Thermal analysis was also performed to study the thermal degradation of BF/PLA composites. The fibre dispersion, orientation, fibre length retention, and fibre damage were also examined during the processing of BF/PLA composite through injection moulding.

## 2 Experimental Details

### 2.1 Materials

The widely available polylactic acid (PLA) was chosen as the matrix, supplied by Natur Tec India Pvt. Ltd. The bamboo fibre (BF) was considered as reinforcement to develop BF/PLA composite, collected from Vruksha Composites Pvt. Ltd., Andhra Pradesh, India. The ranges of melting and glass transition temperatures of PLA are between 145–180 °C and 50–80 °C. Before the chemical treatment, the fibres were thoroughly washed and dried. Unwanted residues were removed from the surface of the fibres by detergent washing. The bamboo fibres were then immersed for 4 h in an aqueous solution containing 2% NaOH [21]. The fibres were again rinsed with distilled water to eliminate remnant impurities. After that, the fibres were dried at ambient temperature and then placed in an oven for the purpose of preheating at 60 °C to remove the remaining moisture. The chemical modification of BF due to treatment is presented in Eq. (1) [21].

$$\text{Fiber} - \text{OH} + \text{NaOH} \rightarrow \text{Fiber} - \text{O} - \text{Na}^{+} + \text{H}_2\text{O} \quad (1)$$

### 2.2 Composite Fabrication

PLA pellets were de-moisturized in an electric oven at 70 °C for 6 h. The chemically modified BF was manually cut to obtain the fibre lengths ($L$) of 2, 3, 4, 5, and 6 mm. Green composites were developed at fibre loadings ($D$) of 10, 20, and 30% (w/w). Both the effect of fibre loading and length on the performance of BF/PLA composite was investigated. A 50-ton servo-controlled hydraulic injection moulding machine was chosen to produce the BF/PLA composite. The barrel temperature in the injection moulding machine was regulated with respect to the experimental plan. The cooling time was considered as 25 s. The injection took place for 2 s (shot size: 20 g). The composites were fabricated by directly feeding the short BF and PLA pellets into the hopper. The composites were tested to find the best combination of fibre length and loading. Further, the injection parameters were optimized considering the different properties of the green composite. Tables 1 and 2 provide the details of chosen injection parameters and the experimental plan, respectively.

### 2.3 Composite Testing

The fabricated green composites (BF/PLA) were tested to evaluate their tensile, flexural, compression, and shear properties in agreement with ASTM D-638, D-790, D-3450, and D-5379. Figure 1 depicts the fabricated green composite samples and the corresponding testing procedure. A universal testing machine (Make: Unitek and Model: 9450) of capacity 50 kN was used for testing purposes. Dedicated compression and shear test fixtures were developed as shown in Fig. 1. Under each experimental condition, the mechanical properties were assessed by testing three samples and the average value was calculated. The morphology of the fractured composite specimens was examined to study the failure behaviour under diverse conditions. FE-SEM (Make: Zeiss and Model: S-3700N) was utilized to study the morphology of the tested specimens. The thermogravimetric analyzer (EXSTAR 6300) was used for the thermal analysis of developed composites. The samples were heated to 650 °C at a steady rate of 10℃ per min in an environment of nitrogen gas (200 mL/min). The distribution and orientation of BF in composites were also examined by using a toolmaker's microscope (Make: Mitutoyo and Model: TM-500 series). The length of the BF was measured using an optical microscope (Make: Olympus and Model: BX51 M).

**Table 1** Injection parameters

| Input parameters | Level-1 | Level-2 | Level-3 |
|---|---|---|---|
| A: Injection pressure (bars) | 70 | 90 | 110 |
| B: Injection speed (mm/s) | 40 | 50 | 60 |
| C: Temperature (°C) | 165 | 175 | 185 |

**Table 2** Experimental layout

| Sl no. | Orthogonal array | | | A: Injection pressure (bars) | B: Injection speed (mm/s) | C: Injection temperature (°C) |
|---|---|---|---|---|---|---|
| 1 | 1 | 1 | 1 | 70 | 40 | 165 |
| 2 | 1 | 2 | 2 | 70 | 50 | 175 |
| 3 | 1 | 3 | 3 | 70 | 60 | 185 |
| 4 | 2 | 1 | 2 | 90 | 40 | 175 |
| 5 | 2 | 2 | 3 | 90 | 50 | 185 |
| 6 | 2 | 3 | 1 | 90 | 60 | 165 |
| 7 | 3 | 1 | 3 | 110 | 40 | 185 |
| 8 | 3 | 2 | 1 | 110 | 50 | 165 |
| 9 | 3 | 3 | 2 | 110 | 60 | 175 |

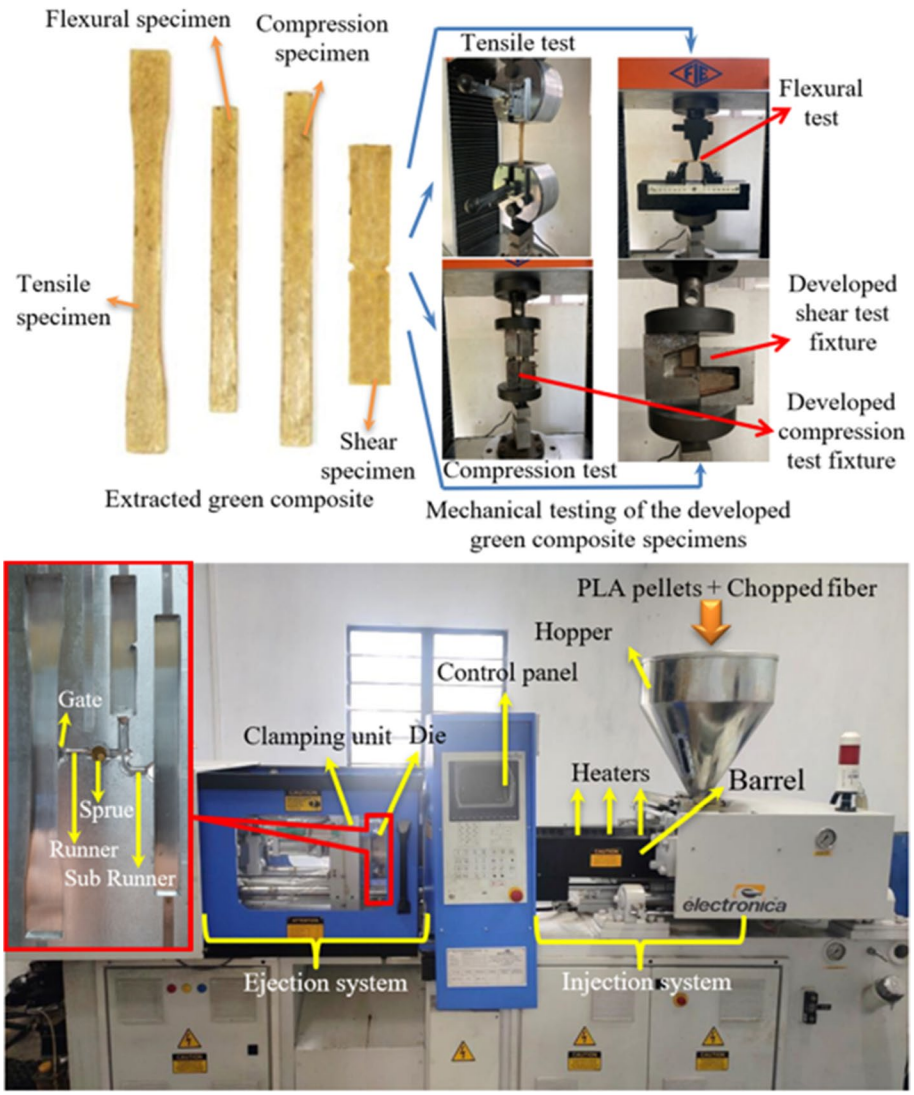


**Fig. 1** Methodology followed to develop the BF/PLA composite

## 3 Results and Discussion

### 3.1 Analysis of Fibre Length and Fibre Loading

Initially, the mechanical properties were evaluated by varying the fabrication parameters (fibre length and fibre loading). The steps involved in GRA are shown in Table 3. The mechanical properties of BF/PLA composite with varying fibre loading and length are presented in Table 4. The calculated normalized and deviation sequence values are presented in Table 5. GRC of tensile and flexural properties were calculated and then GRG was calculated considering the average of each trial (Table 6).

The highest GRG represents the optimal parameter setting. The optimal parameter setting was L3-D2 (4 mm and 20%). ANOVA was accomplished to further confirm the optimal level. From the means plot, the optimal level was found as *L*3–*D*1 (4 mm and 10%). The optimal parameter setting achieved from the means plot and GRG was different. Therefore, the results were compared to confirm the optimal level as *L*3–*D*2. The highest GRG was calculated as 0.7775.

### 3.2 Analysis of Injection Parameters

BF/PLA composites were further fabricated at optimum fabrication parameter conditions i.e., considering the fibre length of 4 mm and fibre loading of 20% to study the effect of injection parameters (injection pressure, injection speed, and injection temperature) on the mechanical properties of BF/PLA composite. $L_9$ orthogonal array was chosen to perform the GRA. The mechanical properties are displayed in Table 7. The calculated normalized, deviation sequence, GRC, GRG, and rank values are represented in Tables 8, 9 and 10. The optimal injection condition to attain superior

**Table 3** Process steps involved in GRA

| Steps | Formula | Designation |
|---|---|---|
| Normalization | $X_i(p) = \frac{X_i^{(0)}(p) - \mathrm{Min}X_i^{(0)}(p)}{\mathrm{Max}X_i^{(0)}(p) - \mathrm{Min}X_i^{(0)}(p)}$ | The output response of each column's is denoted by $X_i^{(0)}(p)$, the lowest output response is signified by $MinX_i^{(0)}(p)$, and the highest output response is symbolized by $MaxX_i^{(0)}(p)$, where I implies to total no. of tests |
| Deviation sequence | $\Delta_{ij} = \left\|X_{oj} - X_{ij}\right\|$ | ideal normalized value is represented with $X_{oj}$ |
| GRC | $\mathrm{GRC}_{ij} = \frac{\Delta_{\min} + \zeta\Delta_{\max}}{\Delta_{oi}(k) + \zeta\Delta_{\max}}$ | The lowest deviation sequence value is denoted with $\Delta_{\min}$, maximum deviation sequence value is presented as $\Delta_{\max}$, individual deviation sequence is signified as $\Delta_{oi}(k)$, and coefficient of constant is $\zeta$ |
| GRG | $\mathrm{GRG} = \frac{1}{m}\sum \mathrm{GRC}_{ij}$ | Grey relational coefficient is denoted with $\mathrm{GRC}_{ij}$ |

**Table 4** Tensile and flexural properties obtained by varying the fabrication parameters

| Expt. no. | Fibre length (mm) | Fibre loading (%) | TS (MPa) | TM (MPa) | FS (MPa) | FM (GPa) |
|---|---|---|---|---|---|---|
| 1 | 2 | 20 | 24 | 417 | 73.81 | 5.04 |
| 2 | 4 | 20 | 32 | 498 | 86.7 | 4.34 |
| 3 | 4 | 10 | 31 | 517 | 83.04 | 3.60 |
| 4 | 5 | 10 | 21 | 462 | 84.26 | 4.56 |
| 5 | 4 | 30 | 19 | 433 | 88.14 | 3.89 |
| 6 | 3 | 20 | 27 | 472 | 87.84 | 5.11 |
| 7 | 3 | 30 | 21 | 419 | 64.59 | 5.60 |
| 8 | 2 | 10 | 33 | 456 | 81.10 | 3.52 |
| 9 | 6 | 20 | 18 | 367 | 86.73 | 3.62 |
| 10 | 5 | 20 | 25 | 430 | 82.30 | 4.19 |
| 11 | 3 | 10 | 29 | 485 | 84.89 | 4.02 |
| 12 | 6 | 30 | 17 | 398 | 76.13 | 3.85 |
| 13 | 5 | 30 | 21 | 402 | 62.01 | 3.19 |
| 14 | 2 | 30 | 15 | 422 | 53.51 | 5.25 |
| 15 | 6 | 10 | 23 | 457 | 80.42 | 4.46 |

**Table 5** Normalized and deviation sequence values of tensile and flexural properties obtained by varying the fabrication parameters

| Expt. no. | Normalization | | | | Deviation sequence | | | |
|---|---|---|---|---|---|---|---|---|
| | TS (MPa) | TM (MPa) | FS (MPa) | FM (GPa) | TS (MPa) | TM (MPa) | FS (MPa) | FM (GPa) |
| 1 | 0.5000 | 0.3333 | 0.5862 | 0.7676 | 0.5000 | 0.6667 | 0.4138 | 0.2324 |
| 2 | 0.9444 | 0.8733 | 0.9584 | 0.4772 | 0.0556 | 0.1267 | 0.0416 | 0.5228 |
| 3 | 0.8889 | 1.0000 | 0.8516 | 0.1701 | 0.1111 | 0.0000 | 0.1484 | 0.8299 |
| 4 | 0.3333 | 0.6333 | 0.8880 | 0.5685 | 0.6667 | 0.3667 | 0.1120 | 0.4315 |
| 5 | 0.2222 | 0.4400 | 1.0000 | 0.2905 | 0.7778 | 0.5600 | 0.0000 | 0.7095 |
| 6 | 0.6667 | 0.7000 | 0.9913 | 0.7967 | 0.3333 | 0.3000 | 0.0087 | 0.2033 |
| 7 | 0.3333 | 0.3467 | 0.3200 | 1.0000 | 0.6667 | 0.6533 | 0.6800 | 0.0000 |
| 8 | 1.0000 | 0.5933 | 0.7938 | 0.1369 | 0.0000 | 0.4067 | 0.2062 | 0.8631 |
| 9 | 0.1667 | 0.0000 | 0.9593 | 0.1784 | 0.8333 | 1.0000 | 0.0407 | 0.8216 |
| 10 | 0.5556 | 0.4200 | 0.8314 | 0.4149 | 0.4444 | 0.5800 | 0.1686 | 0.5851 |
| 11 | 0.7778 | 0.7867 | 0.9062 | 0.3444 | 0.2222 | 0.2133 | 0.0938 | 0.6556 |
| 12 | 0.1111 | 0.2067 | 0.6532 | 0.2739 | 0.8889 | 0.7933 | 0.3468 | 0.7261 |
| 13 | 0.3333 | 0.2333 | 0.2452 | 0.0000 | 0.6667 | 0.7667 | 0.7548 | 1.0000 |
| 14 | 0.0000 | 0.3667 | 0.0000 | 0.8548 | 1.0000 | 0.6333 | 1.0000 | 0.1452 |
| 15 | 0.4444 | 0.6000 | 0.7771 | 0.5270 | 0.5556 | 0.4000 | 0.2229 | 0.4730 |

**Table 6** GRC, grade, and rank of tensile and flexural properties obtained by varying the fabrication parameters

| Expt. no. | TS (MPa) | TM (MPa) | FS (MPa) | FM (GPa) | Grade | Rank |
|---|---|---|---|---|---|---|
| 1 | 0.5000 | 0.4286 | 0.5472 | 0.6827 | 0.5396 | 11 |
| 2 | 0.9000 | 0.7979 | 0.9232 | 0.4888 | 0.7775 | 1 |
| 3 | 0.8182 | 1.0000 | 0.7711 | 0.3760 | 0.7413 | 2 |
| 4 | 0.4286 | 0.5769 | 0.8169 | 0.5367 | 0.5898 | 6 |
| 5 | 0.3913 | 0.4717 | 1.0000 | 0.4134 | 0.5691 | 8 |
| 6 | 0.6000 | 0.6250 | 0.9830 | 0.7109 | 0.7297 | 3 |
| 7 | 0.4286 | 0.4335 | 0.4237 | 1.0000 | 0.5715 | 7 |
| 8 | 1.0000 | 0.5515 | 0.7080 | 0.3668 | 0.6566 | 5 |
| 9 | 0.3750 | 0.3333 | 0.9247 | 0.3783 | 0.5028 | 12 |
| 10 | 0.5294 | 0.4630 | 0.7478 | 0.4608 | 0.5502 | 10 |
| 11 | 0.6923 | 0.7009 | 0.8420 | 0.4327 | 0.6670 | 4 |
| 12 | 0.3600 | 0.3866 | 0.5905 | 0.4078 | 0.4362 | 14 |
| 13 | 0.4286 | 0.3947 | 0.3985 | 0.3333 | 0.3888 | 15 |
| 14 | 0.3333 | 0.4412 | 0.3333 | 0.7749 | 0.4707 | 13 |
| 15 | 0.4737 | 0.5556 | 0.6916 | 0.5139 | 0.5587 | 9 |

**Table 7** Mechanical properties obtained by varying the injection parameters

| Expt. no. | A | B | C | TS (MPa) | TM (MPa) | $PE_T$ (%) | FS (MPa) | FM (GPa) | $PE_F$ (%) | CS (MPa) | SS (MPa) |
|---|---|---|---|---|---|---|---|---|---|---|---|
| 1 | 70 | 40 | 165 | 27 | 467 | 5.82 | 43.46 | 3.15 | 2.42 | 51 | 17 |
| 2 | 70 | 50 | 175 | 23 | 449 | 6.64 | 96.12 | 2.83 | 1.96 | 63 | 14 |
| 3 | 70 | 60 | 185 | 19 | 333 | 5.42 | 65.62 | 3.36 | 1.84 | 43 | 13 |
| 4 | 90 | 40 | 175 | 26 | 403 | 7.88 | 67.50 | 5.01 | 2.09 | 89 | 15 |
| 5 | 90 | 50 | 185 | 24 | 397 | 5.22 | 70.21 | 5.82 | 2.11 | 86 | 12 |
| 6 | 90 | 60 | 165 | 34 | 498 | 6.71 | 87.20 | 4.43 | 1.76 | 97 | 24 |
| 7 | 110 | 40 | 185 | 23 | 378 | 4.97 | 69.50 | 3.29 | 1.06 | 76 | 19 |
| 8 | 110 | 50 | 165 | 31 | 504 | 6.48 | 93.01 | 6.17 | 1.57 | 83 | 17 |
| 9 | 110 | 60 | 175 | 28 | 524 | 5.97 | 89.24 | 5.31 | 1.91 | 79 | 16 |

**Table 8** Normalized mechanical properties obtained by varying the injection parameters

| Expt. no. | TS (MPa) | TM (MPa) | $PE_T$ (%) | FS (MPa) | FM (GPa) | $PE_F$ (%) | CS (MPa) | SS (MPa) |
|---|---|---|---|---|---|---|---|---|
| 1 | 0.5333 | 0.7016 | 0.2921 | 0.0000 | 0.0958 | 1.0000 | 0.1481 | 0.4167 |
| 2 | 0.2667 | 0.6073 | 0.5739 | 1.0000 | 0.0000 | 0.6618 | 0.3704 | 0.1667 |
| 3 | 0.0000 | 0.0000 | 0.1546 | 0.4208 | 0.1587 | 0.5735 | 0.0000 | 0.0833 |
| 4 | 0.4667 | 0.3665 | 1.0000 | 0.4565 | 0.6527 | 0.7574 | 0.8519 | 0.2500 |
| 5 | 0.3333 | 0.3351 | 0.0859 | 0.5080 | 0.8952 | 0.7721 | 0.7963 | 0.0000 |
| 6 | 1.0000 | 0.8639 | 0.5979 | 0.8306 | 0.4790 | 0.5147 | 1.0000 | 1.0000 |
| 7 | 0.2667 | 0.2356 | 0.0000 | 0.4945 | 0.1377 | 0.0000 | 0.6111 | 0.5833 |
| 8 | 0.8000 | 0.8953 | 0.5189 | 0.9409 | 1.0000 | 0.3750 | 0.7407 | 0.4167 |
| 9 | 0.6000 | 1.0000 | 0.3436 | 0.8694 | 0.7425 | 0.6250 | 0.6667 | 0.3333 |

**Table 9** Deviation sequence of mechanical properties obtained by varying the injection parameters

| Expt. no. | TS (MPa) | TM (MPa) | $PE_T$ (%) | FS (MPa) | FM (GPa) | $PE_F$ (%) | CS (MPa) | SS (MPa) |
|---|---|---|---|---|---|---|---|---|
| 1 | 0.4667 | 0.2984 | 0.7079 | 1.0000 | 0.9042 | 0.0000 | 0.8519 | 0.5833 |
| 2 | 0.7333 | 0.3927 | 0.4261 | 0.0000 | 1.0000 | 0.3382 | 0.6296 | 0.8333 |
| 3 | 1.0000 | 1.0000 | 0.8454 | 0.5792 | 0.8413 | 0.4265 | 1.0000 | 0.9167 |
| 4 | 0.5333 | 0.6335 | 0.0000 | 0.5435 | 0.3473 | 0.2426 | 0.1481 | 0.7500 |
| 5 | 0.6667 | 0.6649 | 0.9141 | 0.4920 | 0.1048 | 0.2279 | 0.2037 | 1.0000 |
| 6 | 0.0000 | 0.1361 | 0.4021 | 0.1694 | 0.5210 | 0.4853 | 0.0000 | 0.0000 |
| 7 | 0.7333 | 0.7644 | 1.0000 | 0.5055 | 0.8623 | 1.0000 | 0.3889 | 0.4167 |
| 8 | 0.2000 | 0.1047 | 0.4811 | 0.0591 | 0.0000 | 0.6250 | 0.2593 | 0.5833 |
| 9 | 0.4000 | 0.0000 | 0.6564 | 0.1306 | 0.2575 | 0.3750 | 0.3333 | 0.6667 |

**Table 10** GRC, grade, and rank of mechanical properties obtained by varying the injection parameters

| Expt. no. | TS (MPa) | TM (MPa) | $PE_T$ (%) | FS (MPa) | FM (GPa) | $PE_F$ (%) | CS (MPa) | SS (MPa) | Grades | Rank |
|---|---|---|---|---|---|---|---|---|---|---|
| 1 | 0.5172 | 0.6262 | 0.4139 | 0.3333 | 0.3561 | 1.0000 | 0.3699 | 0.4615 | 0.5098 | 7 |
| 2 | 0.4054 | 0.5601 | 0.5399 | 1.0000 | 0.3333 | 0.5965 | 0.4426 | 0.3750 | 0.5316 | 6 |
| 3 | 0.3333 | 0.3333 | 0.3716 | 0.4633 | 0.3728 | 0.5397 | 0.3333 | 0.3529 | 0.3875 | 9 |
| 4 | 0.4839 | 0.4411 | 1.0000 | 0.4792 | 0.5901 | 0.6733 | 0.7714 | 0.4000 | 0.6049 | 4 |
| 5 | 0.4286 | 0.4292 | 0.3536 | 0.5040 | 0.8267 | 0.6869 | 0.7105 | 0.3333 | 0.5341 | 5 |
| 6 | 1.0000 | 0.7860 | 0.5543 | 0.7470 | 0.4897 | 0.5075 | 1.0000 | 1.0000 | 0.7606 | 1 |
| 7 | 0.4054 | 0.3954 | 0.3333 | 0.4973 | 0.3670 | 0.3333 | 0.5625 | 0.5455 | 0.4300 | 8 |
| 8 | 0.7143 | 0.8268 | 0.5096 | 0.8944 | 1.0000 | 0.4444 | 0.6585 | 0.4615 | 0.6887 | 2 |
| 9 | 0.5556 | 1.0000 | 0.4324 | 0.7928 | 0.6601 | 0.5714 | 0.6000 | 0.4286 | 0.6478 | 3 |

mechanical properties were noticed as A2–B3–C1 (injection pressure: 90 bars, injection speed: 60 mm/s, and injection temperature: 165 °C). Subsequently, the optimal condition obtained from the mean plots was the same. The maximum GRG value was calculated as 0.7606.

### 3.3 Analysis of Variance

The fabrication parameters (fibre length and fibre loading) and injection parameters (pressure, speed, and temperature) affecting the mechanical properties of BF/PLA composites were inspected by performing ANOVA of GRG. The proposed statistical model was validated by a test for normality and equal variance. The results of the normality test are graphically depicted in Figs. 2 and 3. The test results revealed that the data is normally distributed. The GRG probability plot indicates that the depicted points are relatively close to the fitted distribution line at a confidence level of 95% ($\leq 0.05$). Anderson–Darling (AD) statistics are quite small for both fabrication parameters (0.240) and injection parameters (0.157). These low values indicate that the data are evenly distributed around the fitted line. The $p$ values for fabrication and injection parameters are 0.729 and 0.926. The $p$ values are more than 0.05. This implies that the null hypothesis cannot be rejected and thus, confirming that the data follow a normal distribution. This can also be noticed

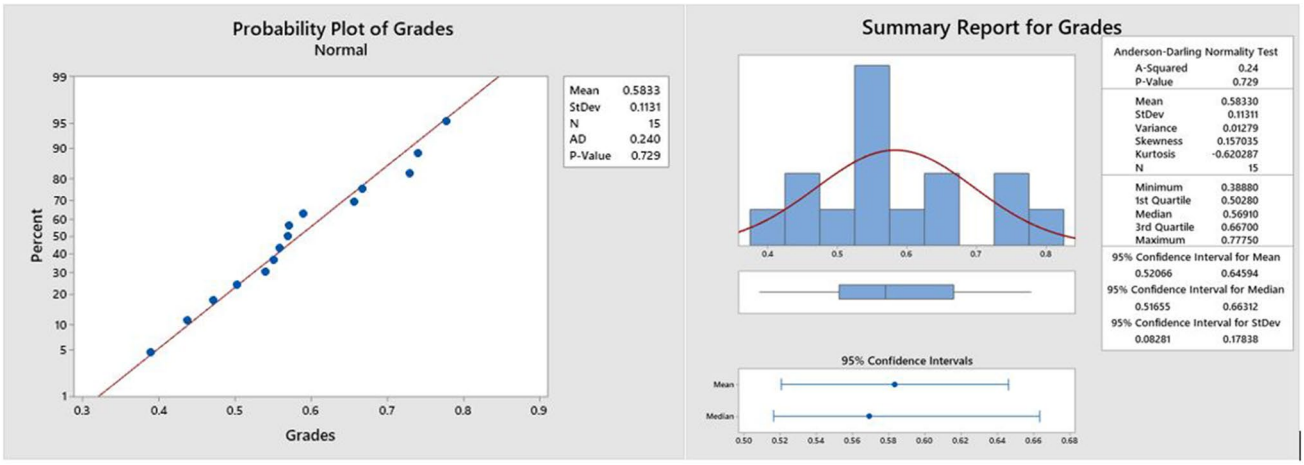


**Fig. 2** Normality test results obtained by varying the fabrication parameters

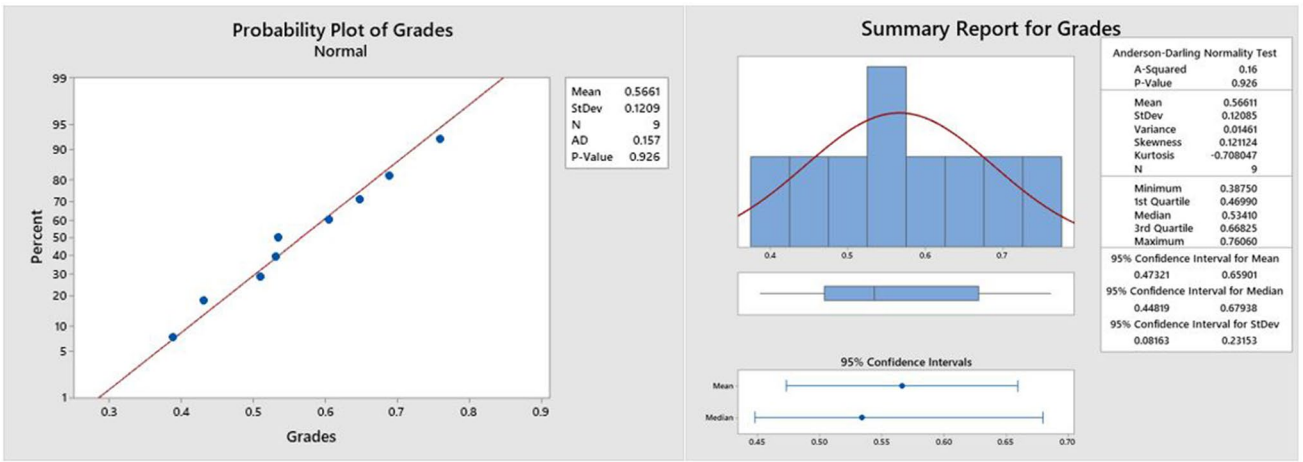


**Fig. 3** Normality test results obtained by varying the injection parameters

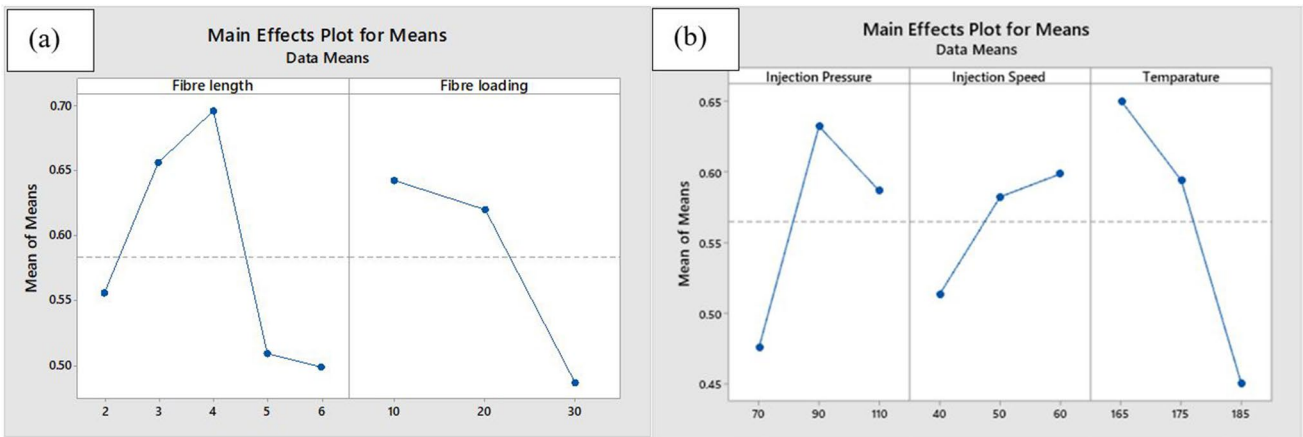


**Fig. 4** Means plot obtained by varying **a** fabrication parameters and **b** injection parameters

**Table 11** ANOVA of GRG for fabrication parameters

| Source | DF | Adj SS | Adj MS | *F*-value | *p* value | % Contribution |
|---|---|---|---|---|---|---|
| Fibre length | 4 | 0.09374 | 0.023436 | 12.60 | 0.002 | 52.33 |
| Fibre loading | 2 | 0.07048 | 0.035242 | 18.95 | 0.001 | 39.35 |
| Residual error | 8 | 0.01488 | 0.001860 | | | |
| Total | 14 | 0.17911 | | | | |

**Table 12** ANOVA of GRG of injection process parameters

| Source | DF | Seq SS | Adj MS | *F* | *p* | % Contribution |
|---|---|---|---|---|---|---|
| Injection pressure | 2 | 0.039234 | 0.019617 | 129.76 | 0.008 | 33.58 |
| Injection speed | 2 | 0.012098 | 0.006049 | 40.01 | 0.024 | 10.35 |
| Temperature | 2 | 0.065187 | 0.032594 | 215.60 | 0.005 | 55.80 |
| Residual error | 2 | 0.000302 | 0.000151 | | | |
| Total | 8 | 0.116822 | | | | |

**Table 13** Model summary of GRG

| Parameters | *S* | *R*-sq | *R*-sq(adj) |
|---|---|---|---|
| Fabrication | 0.0431288 | 94.69% | 89.46% |
| Injection | 0.01230 | 99.7% | 99.0% |

from the histogram shown in Figs. 2 and 3. Attainment of lower A-squared values further validates the certainty of normality. The results showed that the *p* values are ≥ 0.05. The data presented was insufficient to reject the null hypothesis of equal variances. The overlapping confidence intervals reflect the significant differences in variances. Figure 4 depicts the mean graphs of GRG for chosen parameters. The optimum levels from mean plots were observed as *L*3–*D*1 (4 mm and 10%) for fabrication parameters and A2–B3–C1 (90 bars, 60 mm/s, and 165 °C) for injection parameters. The contribution of these parameters is presented in Tables 11 and 12. The *p* values for the fibre length and loading are 0.002 and 0.001 (≤ 0.05). Whereas the *p* values of injection pressure, injection speed, and injection temperature are 0.008, 0.024, and 0.005. The percentage contribution of fibre length and fibre loading was 52.33% and 39.35%. Whereas the percentage contribution of injection pressure, injection speed, and injection temperature are 33.58%, 10.35%, and 55.80%. The model summary of fabrication and injection parameters is represented in Table 13. *R*-square values were found as 94.69% and 99.70% for fabrication and injection parameters. The higher *R*-squared value indicates a better fit between the data and the model.

### 3.4 Confirmation Test

The confirmation test was performed to find the selection of the best set of process parameters. The experimental and predicted GRG were compared. The predicted GRG was calculated using Eq. (2).

$$r^{\wedge} = r_{\mathrm{m}} + \sum_{i=1}^{q}(r - r_{\mathrm{m}}) \tag{2}$$

Here, $r_{\mathrm{m}}$ implies the average of means of grades, $r$ denotes the mean of grades at optimal level, and q is the number of input parameters. The actual and predicted GRG obtained at the optimal condition is summarised in Table 14. The actual and predicted GRG values are 0.7775 and 0.7555 for varying fabrication parameters. GRG showed an improvement of 0.022. The actual and predicted GRG for the injection parameters were 0.7606 and 0.7526, respectively. Here, GRG improvement was 0.008.

### 3.5 Thermal Analysis

The thermal analysis was conducted to compare the thermal performance of pure PLA with the developed BF/PLA composites (both Rank 1 and Rank 9). Rank 1

**Table 14** Comparison of experimental and predicted GRG values

| Parameters | Optimum level | GRG | Improvement |
|---|---|---|---|
| Fabrication parameters | Experimental (L3-D2) | 0.7775 (Rank 1) | 0.022 |
| | Means plot (L3-D1) | 0.7555 (Predicted) | |
| Injection parameters | Experimental (A2-B3-C1) | 0.7606 (Rank 1) | 0.008 |
| | Means plot (A2-B3-C1) | 0.7526 (Predicted) | |

(highest GRG) represents the injection condition under which the best properties were achieved. Whereas Rank 9 represents the condition at which the properties of the composites were poor. The thermogravimetric analysis (TGA) was performed at 10 °C/min in the temperature range of 30–650 °C. The temperature range in the first phase was 30–100 °C, where the moisture present in BF was evaporated. The initial degradation started in the temperature range of 100–130 °C. The small decrement in the peaks with respect to the time indicates that the hydrophobicity of the BF was improved, as shown in Fig. 5b [22]. The second phase attributed to decomposition, which was in the temperature range of 130–410 °C. The degradation of BF/PLA composite was noticed in the temperature range of 220–390 °C. The peak degradation for PLA was observed at 382 °C. For Rank 1 and Rank 9 composites, peak degradation was noticed at 348 °C and 343 °C. Both cellulose and hemicellulose degraded thermally in the second phase. The thermal stability of PLA was better than the BF (20%)/PLA composite. The addition of BF resulted in breaking the polymeric chains of PLA, which caused early degradation. Also, the thermal stability of Rank 1 composite was better than Rank 9 composite. The low injection pressure and high melting temperature detrimentally affected the thermal stability of the composite secured Rank 9. The low injection pressure caused poor interfacial bonding between the PLA and BF whereas the high melting temperature resulted in an initial degradation of the composite constituents. The thermal stability of lignin is more than cellulose and hemicellulose. The thermal degradation of lignin and other components was predominant in the third phase where the temperature range was 420–650 °C [22, 23]. The remaining in the third phase can be noticed as char and ash.

### 3.6 Morphological Analysis

In this study, BF was chemically treated with 2%NaOH for 4 h. as superior mechanical properties of BF/PLA composite were obtained at this condition [21]. Figures 6 and 7 represent the FESEM images of Rank 1 and Rank 9 composite specimens. The better mechanical properties were attained at the injection parameter setting of 90 bars, 60 mm/s, and 165 °C (Rank 1). The properties were relatively poor at the injection condition of 70 bars, 60 mm/s, and 185 °C (Rank 9). The common damages observed during mechanical testing of short fibre-reinforced composites are (a) fibre breakage, (b) microcrack formation, (c) fibre pull-outs, (d) matrix cracking, (e) fibre crushing, (f) fibre bending, and (g) microfibril formation. Comparatively less fibre pull-outs and crack formations were noticed under tensile loading as shown in Fig. 6a. Fibre tips inside the matrix were a clear indication of proper adhesion. Irregular cracks on the fibre and fibre pull-outs were observed in Rank 1 composite under flexural loading (Fig. 6b). Here, debonding was not observed between the matrix and fibre which resulted in better flexural properties. Fibre bending coupled with microcrack on the fibre surface was observed under compression loading, as shown in Fig. 6c. The surface morphology of the fractured specimen under compression loading showed a good affinity between the matrix and fibre. The fibre pull-outs and cracks on the matrix were noticed under shear loading, though debonding was not observed (Fig. 6d). The composite fabricated under optimal injection conditions showed a better affinity between the constituents due to the proper combination of injection parameters. The proper melting and blending resulted in better adhesion between the BF and PLA at the injection temperature of 165 °C [24]. The injection pressure of 90 bars and the injection speed of 60 mm/s was an excellent combination to disperse the fibre uniformly throughout the matrix. More fibre pull-outs coupled with

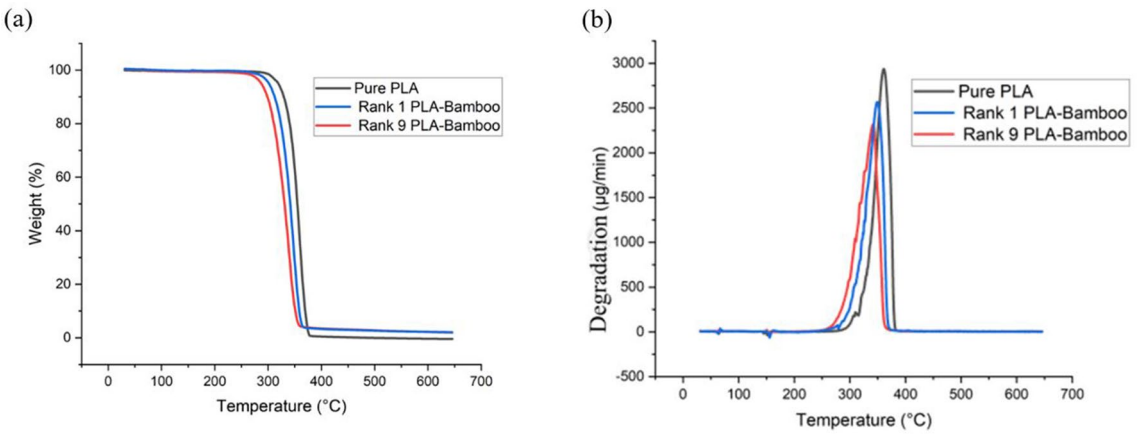


**Fig. 5** Thermal analysis of BF/PLA composite **a** TGA and **b** DTG

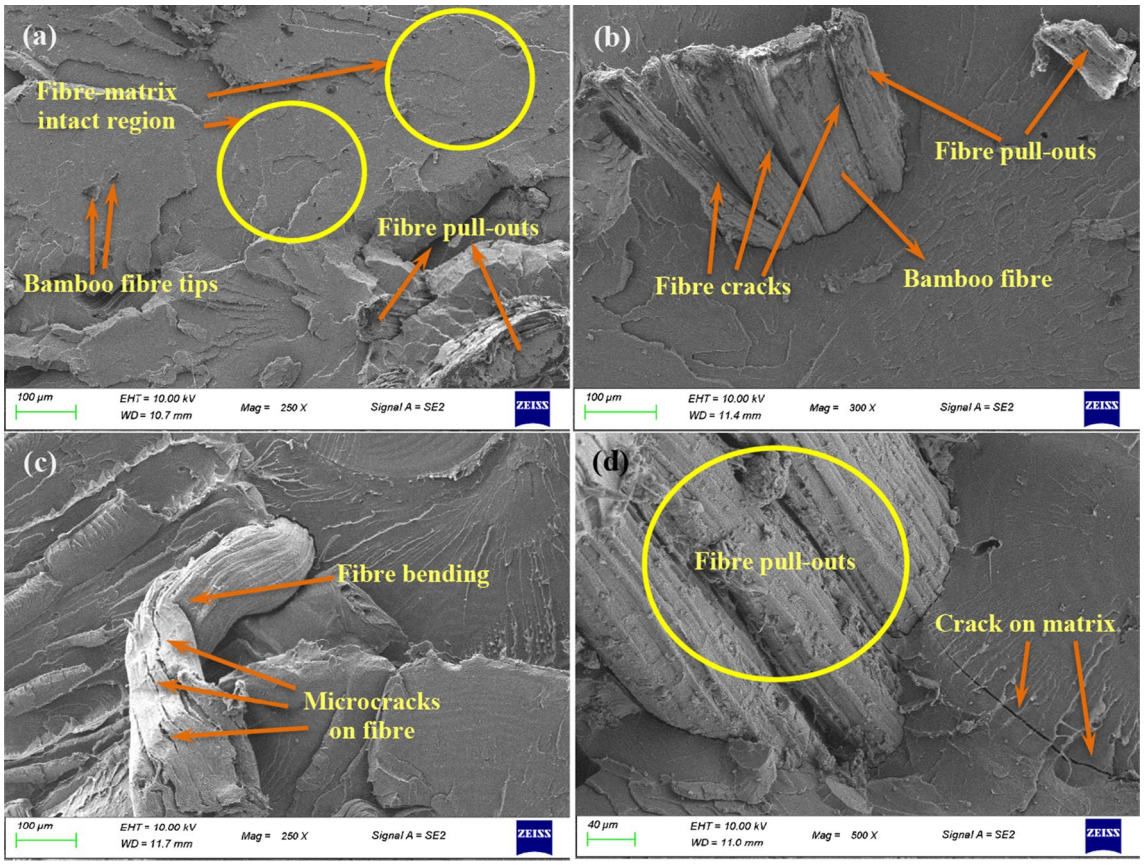


**Fig. 6** FE-SEM images of fractured specimens of Rank 1 composite obtained under **a** tensile, **b** flexural, **c** compression, and **d** shear loadings

debonding were noticed under tensile loading for the Rank 9 composite specimen, as shown in Fig. 7a. The less injection pressure (70 bars) resulted in poor adhesion among the constituents. Furthermore, initial degradation of fibre or matrix may occur due to the high temperature (185 °C) [25]. Fibre pull-outs, microcracks formation, and crack at the fibre tips were detected under flexural loading (Fig. 7b). The major damage modes under compression loading were fibre crushing, microcracks, and microfibrils formation, as shown in Fig. 7c. Whereas more fibre pull-outs coupled with debonding between the BF and PLA were noticed under shear loading (Fig. 7d).

### 3.7 Analysis of Fibre Dispersion and Orientation

PLA and BF mixture was fed into the hopper for the purpose of melting and blending inside the heated barrel. The material mixture reached the nozzle chamber with the help of a reciprocating screw. The screw head pushes the material into the die cavity at a certain injection speed and pressure via sprue bushing, as shown in Fig. 8. The extracted sample and direction of material flow are shown in Fig. 9. The die cavity consists of sprue, runner, sub-runner, and gate. In this study, the fibre dispersion and orientation were investigated at the top and midplane of the composite samples. Initially, the milling operation was performed using an end mill cutter to remove the materials so as to obtain the midplane for the purpose of examination. But the surface was not clearly visible under the microscope due to the exposure of fibre during the milling operation. Hence, the fibre dispersion and orientation in the midplane were studied by mechanically cutting the specimen using a firmer chisel as a better surface was obtained for examination under the microscope. The fibre dispersion and orientation were examined at three different zones of the specimen, as shown in Fig. 9. The fibre dispersion and orientation of BF/PLA composite (Rank 1 and Rank 9) at the different zones for both top and midplane were shown in Figs. 10 and 11. In the Rank 1 composite, the fibre was uniformly distributed (randomly oriented) throughout the matrix in the sprue region (Zone I). Rank 9 composite also showed similar dispersion and orientation of BF. The uniform distribution of BF was also noticed in the top and midplane of the Rank 1 composite in Zone II. However, fibre distribution was nonuniform for the Rank 9 composite in the same zone. In Zone III, the fibre distribution was nonuniform for both Rank 1 and Rank 9 composite.

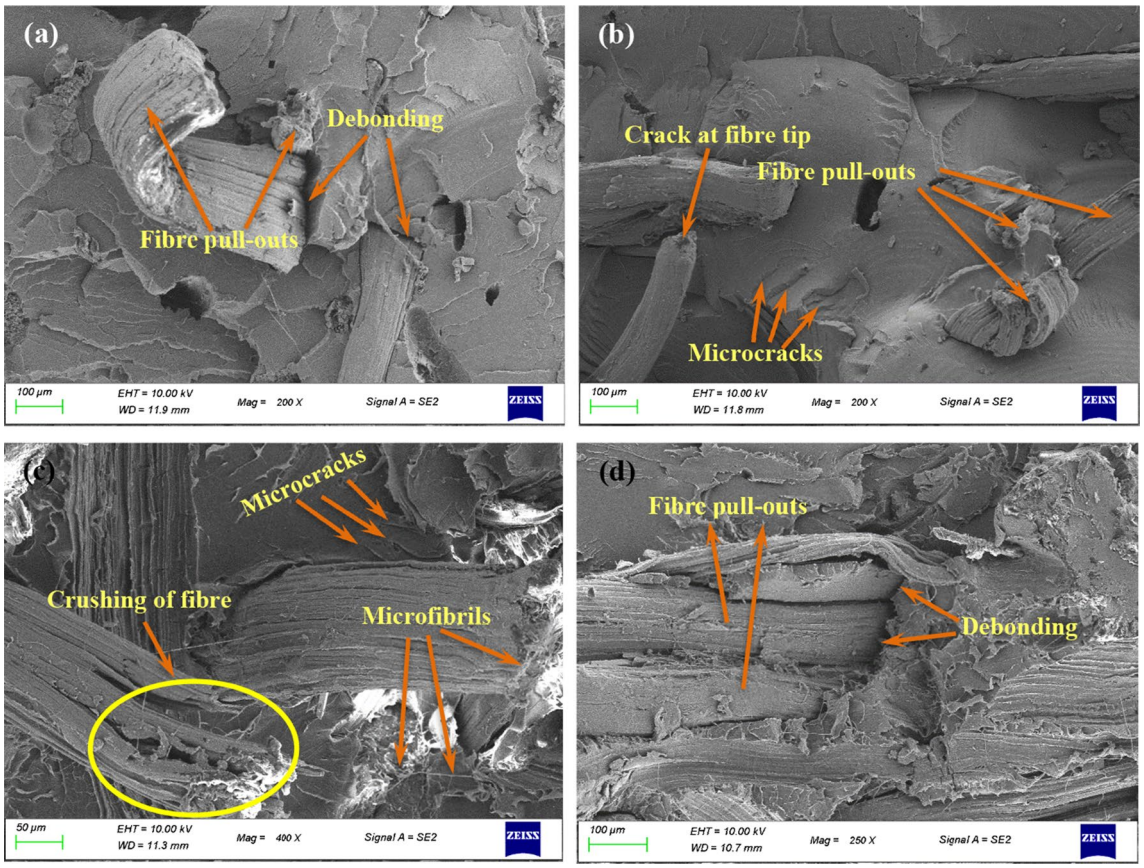


**Fig. 7** FE-SEM images of fractured specimens of Rank 9 composite obtained under **a** tensile, **b** flexural, **c** compression, and **d** shear loadings

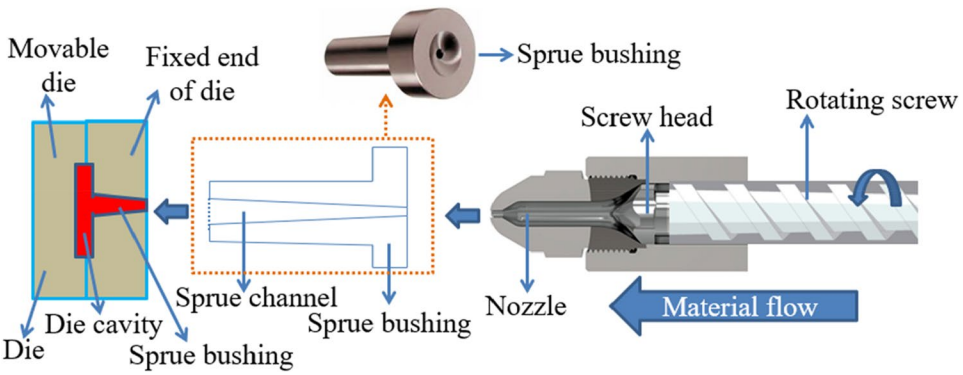


**Fig. 8** Injection of material mixture into die cavity

This is plausibly due to the inadequate injection pressure which caused nonuniform fibre dispersion and orientation for the Rank 9 composite.

### 3.8 Analysis of Fibre Length and Fibre Damage

The composite constituents were separated by dissolving the BF/PLA specimens in an acetone solution to measure the variations in fibre length. The change in fibre length was measured using an optical microscope for both Rank 1 and Rank 9 composites. After dissolving the specimens, 150 fibre samples were collected and then fibre length retention (%) was calculated. Figure 12 shows the measurement of the fibre length. The original fibre length was 4 mm. The change in fibre length was measured and the retention of the fibre length in percentage is displayed in Fig. 13. In the Rank 1 composite, the original fibre length retention was 59.3%. Whereas in the Rank 9 composite, the fibre retention was 54.6%. This indicates that the fibre retention in Rank 9 is less than the Rank 1 composite. The

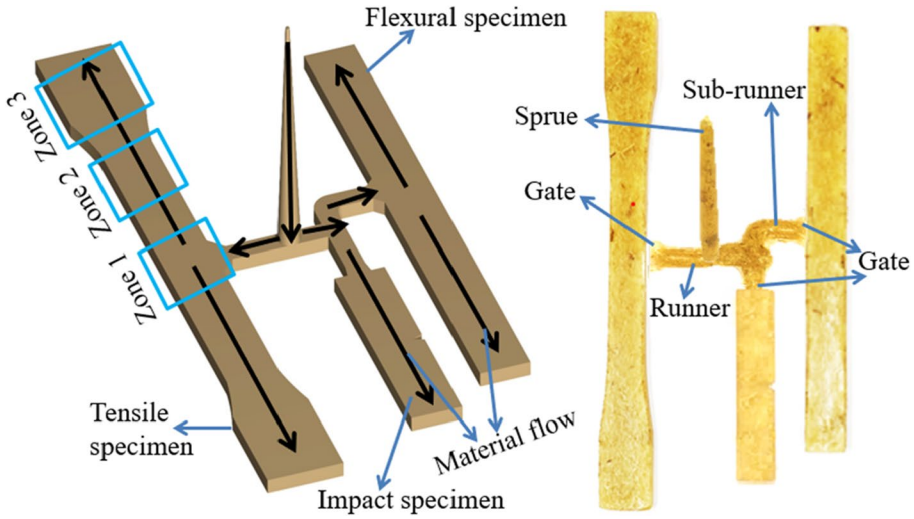


**Fig. 9** Extracted composite specimen and zones considered to study the fibre characteristics

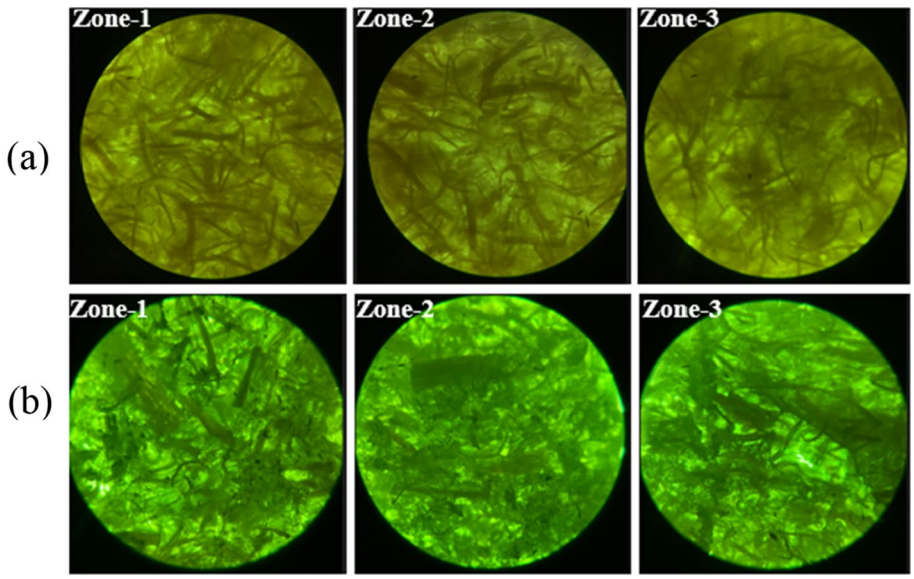


**Fig. 10** Dispersion and orientation of fibre in Rank 1 composite **a** top and **b** midplane

high processing temperature and injection speed damaged the fibre which resulted in comparatively less retention of fibre length for the Rank 9 composite. Also, more fibre damages were noticed in Rank 9 than Rank 1 composite. The major fibre damages were observed as microfibrils formation, cracks at the fibre tip, splitting and crushing of fibre, and fibre bending as shown in Fig. 14.

## 4 Conclusion

In this study, the effect of fabrication parameters and injection parameters on the mechanical properties of the BF/PLA composite was investigated. The major findings from the experimental and statistical analysis are summarized below:

1. The reliability of the statistical model was checked by using the normality and equal variance tests. The established statistical model showed normally distributed data. *R*-sq. values for fabrication and injection parameters were recorded as 94.69% and 99.70%, respectively. The higher *R*-sq. values indicate that the data adequately fit the proposed model.
2. The optimal fabrication parameters combination was *L*3–*D*2 (fibre length: 4 mm and fibre loading: 20%). Meanwhile, the optimum injection parameters were found as A2–B3–C1 (injection pressure: 90 bars, injection speed: 60 mm/s, and injection temperature: 165 °C).
3. The actual and predicted GRG values were obtained as 0.7775 and 0.7555 with an improvement of 0.022 for fabrication parameters. For injection parameters, the

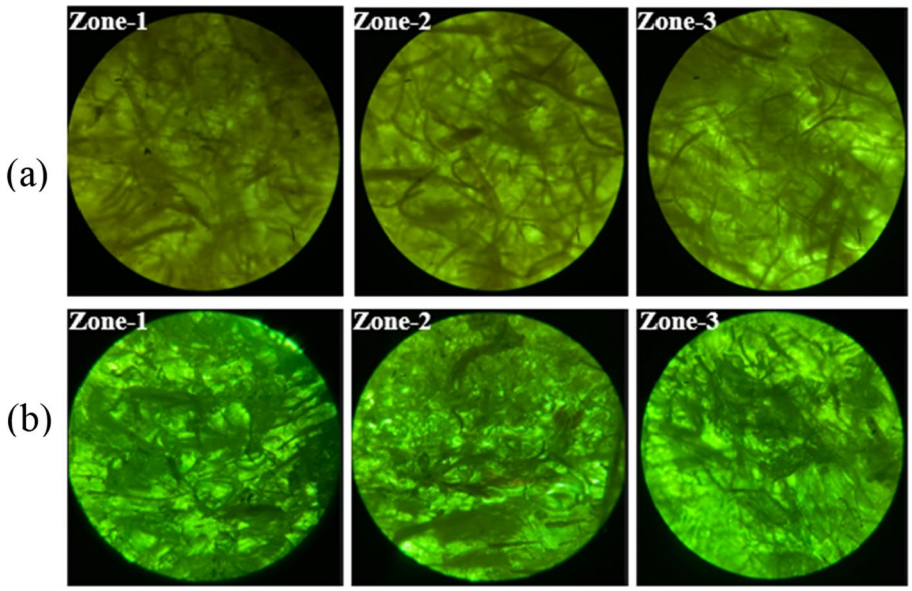


**Fig. 11** Dispersion and orientation of fibre in Rank 9 composite **a** top and **b** midplane

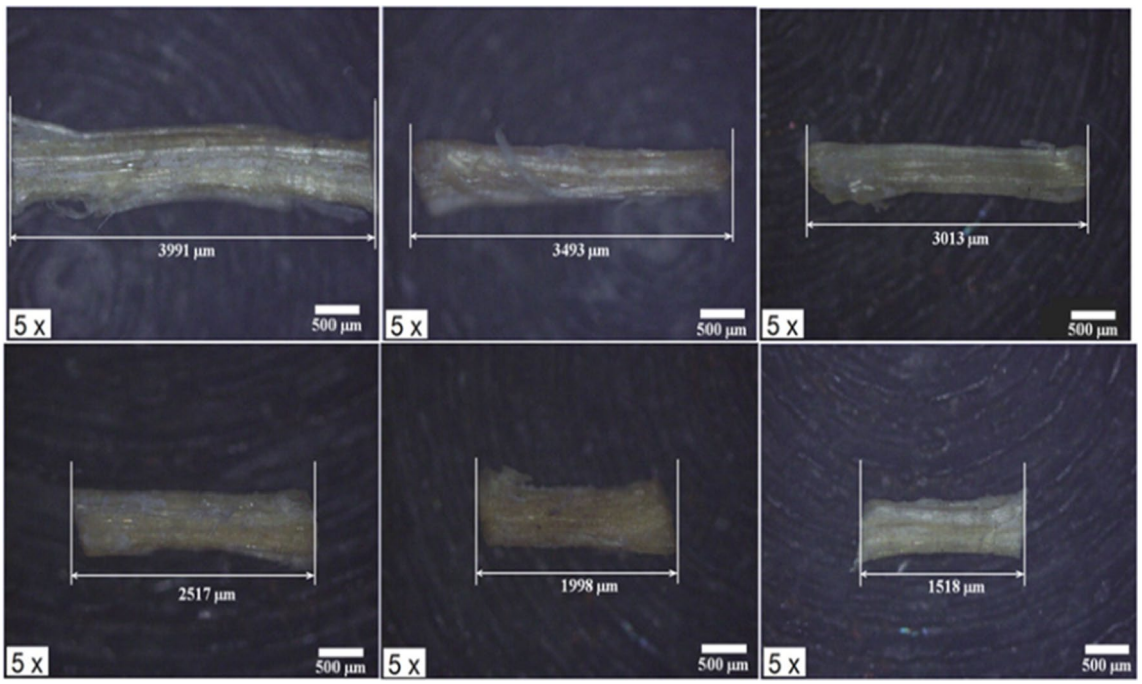


**Fig. 12** Measurement of fibre lengths

values were calculated as 0.7606 and 0.7526 with an improvement of 0.008.

4. ANOVA revealed that all the chosen fabrication and injection parameters are significant as the *p* values are less than 0.05. The contribution of fibre length and fibre loading was 52.33% and 39.35%. Whereas the contribution of the injection pressure, injection speed, and injection temperature was 33.58%, 10.35%, and 55.80%.
5. Through thermal analysis peak degradation for PLA was found at 382 °C. Meanwhile, for Rank 1 and Rank 9 composites, the peak degradation was noticed at 348 °C and 343 °C. The thermal stability of pure PLA was found better than the BF (20%)/PLA composite.
6. The morphology of the fractured specimens showed that the Rank 1 composite specimen exhibited strong bonding between the PLA and BF under different loadings with fewer microcracks, fibre pull-outs, fibre

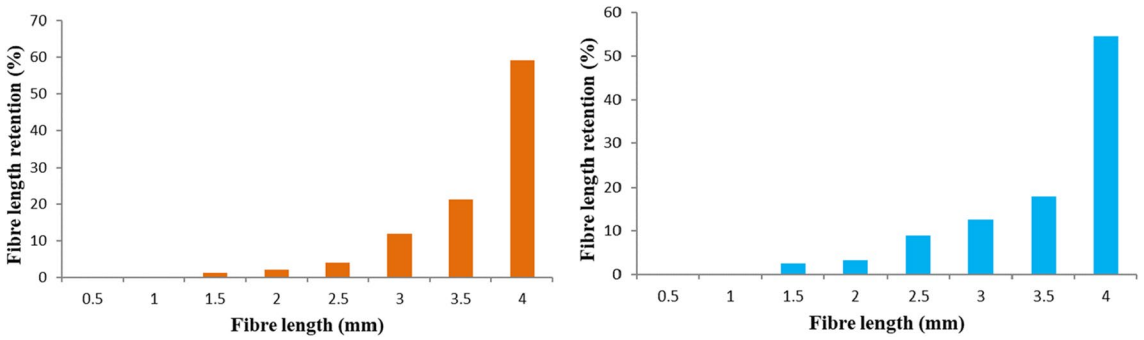


**Fig. 13** Fibre length retention vs. fibre length **a** Rank 1 and **b** Rank 9 composites

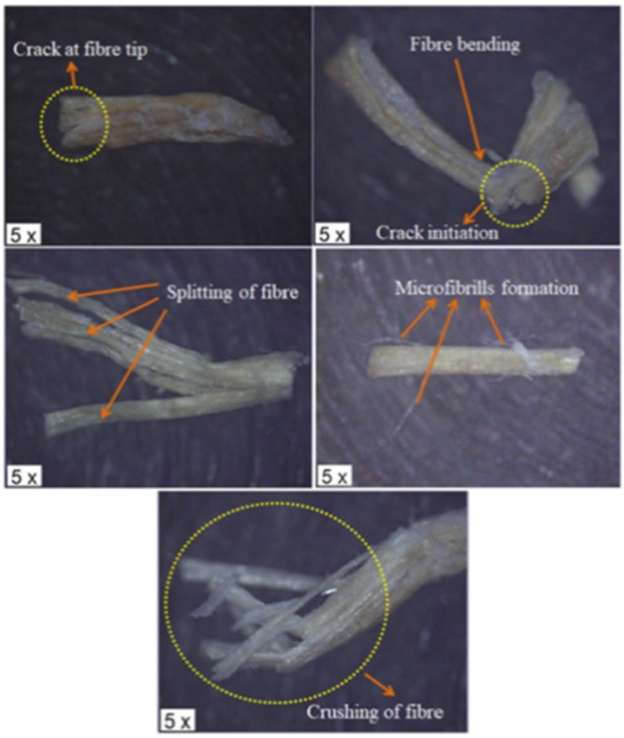


**Fig. 14** Damage to the fibre

breakages, and debonding. However, the Rank 9 composite specimen exhibited more damage due to weak affinity between the constituents.

7. In the Rank 1 composite, the optimal injection parametric condition resulted in better fibre dispersion and orientation. In the Rank 9 composite, improper fibre dispersion and orientation were observed in the different zones of the specimen.
8. The original fibre length retention in the Rank 1 composite was 59.3%. The fibre fraction in the Rank 9 composite was relatively low (54.6%) due to the higher melting temperature and injection speed.
9. The present study investigates the importance of fabrication and injection parameters in developing green composites with superior mechanical and thermal properties. The current work also reveals the future possibilities for the development of high-performance green composites that can replace conventional synthetic composites.
10. According to the current findings, the developed BF/PLA green composite can be used for various applications such as window frames, door panels, mirror casing, table cardboard, household items, storage, and food-packing applications.

**Author Contributions** GSR performed writing—original draft preparation, methodology, and conceptualization. KD accomplished supervision, writing—reviewing and editing, methodology, and conceptualization. RNM performed writing—reviewing and editing.

**Funding** The authors confirm that not received any funds, grants, or other assistance for the preparation of this article.

**Data and Code Availability** Not applicable.

## Declarations

**Conflict of interest** The authors declare no conflicts of interest. All co-authors have seen and agree with the contents of the manuscript, and there is no financial interest to report.

**Ethical approval** Not applicable.

## References

1. S. Joseph, K. Joseph, S. Thomas, Int. J. Polym. Mater. Polym. Biomater. **55**(11), 925–945 (2006)
2. T.A. Negawo, Y. Polat, A. Kilic, Compos. Sci. Technol. **213**, 108937 (2021)
3. Y. Arao, T. Fujiura, S. Itani, T. Tanaka, Compos. Part B Eng. **68**, 200–206 (2015)
4. T. Lemaire, E.G. Rodi, V. Langlois, E. Renard, V. Sansalone, Polymers **13**(16), 2650 (2021)

5. A. Sirichalarmkul, S. Kaewpirom, J. Appl. Polym. Sci. **138**(27), 50652 (2021)
6. M. Barczewski, J. Andrzejewski, R. Majchrowski, K. Dobrzycki, K. Formela, J. Renew. Mater. **9**(5), 841 (2021)
7. F. Kucuk, S. Sismanoglu, Y. Kanbur, U. Tayfun, Clean. Eng. Technol. **4**, 100251 (2021)
8. D. Zindani, S. Kumar, S.R. Maity, S. Bhowmik, J. Polym. Environ. **29**(1), 143–155 (2021)
9. Z. Sun, H. Han, G. Dai, J. Reinf. Plast. Compos. **29**, 637–649 (2009)
10. K. Zhang, V. Nagarajan, N. Zarrinbakhsh, A.K. Mohanty, M. Misra, Macromol. Mater. Eng. **299**(4), 436–446 (2014)
11. R. Muthuraj, M. Misra, A.K. Mohanty, A.C.S. Sustain, Chem. Eng. **3**(11), 2767–2776 (2015)
12. S. Subyakto, E. Hermiati, N. Masruchin, I. Ismadi, K.W. Prasetiyo, W.B. Kusumaningrum, B. Subiyanto, Wood Res. J. **2**(1), 21–26 (2011)
13. B. Bax, J. Müssig, Compos. Sci. Technol. **68**(7–8), 1601–1607 (2008)
14. S. Chaitanya, I. Singh, Mater. Manuf. Proc. **32**(5), 468–474 (2017)
15. A. Koffi, D. Koffi, L. Toubal, Polym. Test. **93**, 106956 (2021)
16. L. Aliotta, V. Gigante, M.B. Coltelli, P. Cinelli, A. Lazzeri, M. Seggiani, Appl. Sci. **9**(18), 3797 (2019)
17. L.J. Rodríguez, M.L. Álvarez-Láinez, C.E. Orrego, J. Appl. Polym. Sci. **139**(3), 51501 (2022)
18. A. Czerniecka-Kubicka, G. Janowski, M. Pyda, W. Frącz, J. Therm. Anal. Calorim. **147**(2), 1017–1029 (2022)
19. H. Dhakal, A. Bourmaud, F. Berzin, F. Almansour, Z. Zhang, D.U. Shah, J. Beaugrand, Ind. Crops Prod. **126**, 394–402 (2018)
20. A. Lekrine, A. Belaadi, A. Makhlouf, S. Amroune, M. Bourchak, H. Satha, M. Jawaid, Mater. Today Commun. **31**, 103574 (2022)
21. S.R. Gorrepotu, K. Debnath, R.N. Mahapatra, J. Polym. Environ. **31**, 1–19 (2022)
22. S. Chaitanya, I. Singh, Int. J. Precis. Eng. Manuf. **5**(1), 143–150 (2018)
23. K.B. Prakash, Y.A. Fageehi, R. Saminathan, P. Manoj Kumar, S. Saravanakumar, R. Subbiah, S. Rajkumar, Adv. Mater. Sci. Eng. **2021**, 1–11 (2021)
24. J.P. Mofokeng, A.S. Luyt, T. Tábi, J. Kovács, J. Thermoplast. Compos. Mater. **25**(8), 927–948 (2012)
25. M. Feldmann, Compos. Part A Appl. Sci. Manuf. **87**, 146–152 (2016)

Springer Nature or its licensor (e.g. a society or other partner) holds exclusive rights to this article under a publishing agreement with the author(s) or other rightsholder(s); author self-archiving of the accepted manuscript version of this article is solely governed by the terms of such publishing agreement and applicable law.